INFLUENCE OF MATERIAL STIFFNESS OF TOTAL HIP PROSTHESIS IN ISOTROPIC BONE-REMODELING PROCESS ANALYSIS

José Eduardo Gubaua

Gabriela Wessling Oening Dicati

Jucélio Tomás Pereira

jose.gubaua@yahoo.com.br

gabyoening@hotmail.com

prof_jucelio_tomas@hotmail.com

Affiliation

Programa de Pós-Graduação em Engenharia Mecânica - Universidade Federal do Paraná.

Av. Cel. Francisco H. dos Santos, 210, Jardim das Américas, 81.531-970, Paraná, Curitiba, Brasil.

Abstract. *Total Hip Arthroplasty (THA) is a surgery that replaces the damaged natural joint by an artificial one composed by biomaterial. This procedure is a bone-adaptation example, which occurs mainly because the change of loading condition applied on femur after THA, loaded by shear forces in interface. The higher material stiffness, the less is the load dissipation in femoral proximal epiphyses. Resorption and apposition cells make the biological adaptation process, replacing damage bone tissue for a new and healthy one. This process is called bone remodeling. Development of mathematical models combined with Finite Element Method (FEM) enable the evaluation of bone tissue behavior. The present study aims the evaluation of bone-remodeling process around total hip prosthesis made by different biomaterials (cobalt-chrome and titanium alloys and a virtual material with Young's modulus similar to cortical bone). FEM is applied coupled with the Stanford isotropic bone-remodeling model in the software Abaqus. The total hip prosthesis is considered totally bonded with host tissue. The results show that flexible materials allow a high dissipation of loads along the interface region, which promotes the bone maintenance. However, it can generate high-levels of stress, mainly in proximal femoral portion, which can cause a bone fracture.*

Keywords: *Bone adaptation, Bone remodeling, Finite Element Method, Abaqus, Biomaterials.*

1 INTRODUCTION

The Total Hip Arthroplasty (THA) is a surgery procedure that replaces the damaged natural joint by an artificial composed by a biomaterial. The importance of the studies on the changes caused by this procedure is reflected on high numbers of procedures made around the world. In several developed countries like German, Switzerland and Denmark, THA has an incidence at least 150 surgical procedures for each 100,000 inhabitants. Thus, around one million of damage hip joints are replaced annually. Besides, THA have annual rate increased 25% between 2000 and 2009. Due to ageing population and growth of the underdeveloped countries, the tendency of THA is to increase on next decades (Holzwarth and Cotogno, 2012). From January 2013 to September 2014, 14,773 surgery procedures were made in Brazil, which results in an increase of 42% in relation to 2012 (Ministério da Saúde, 2014).

The changes in microstructure that occurs in bone tissue after the THA is a clear example of bone adaptation. Bone adaptation occurs predominantly by the modification of load dissipation along the bone/prosthesis interface. Before the surgery procedure, the bone cross section is totally loaded. After the THA, loads are applied on prosthesis, which transmits them along the interface region, mainly, by shear forces. Thus, the load dissipation in interface region is made by material of the prosthesis. The higher stiffness, the less the load dissipation in host tissue of proximal region, which can result in a high-level bone resorption. The regions along the interface with decrease of density value characterized the phenomenon called stress shielding.

Several studies have been done in order to evaluate the bone tissue behavior around cementless femoral prosthesis. Huiskes et al. (1989) present a pioneer study where is evaluated a two-dimensional femoral cementless prosthesis model, composed by different materials. Authors evaluate the load dissipation along the interface and investigate the relation between the stress distribution and prosthesis design related to the problems that can happen. The results obtained show that materials with high stiffness cause more resorption points along interface region, but mainly in proximal portion of the femur. Other aspect is the flexible materials, which allow a better level of load dissipation in proximal region, that causes bone maintenance and a high level of stress, resulting on bone fail. On a follow study, Huiskes et al. (1992) use three-dimensional elements to evaluate the stress shielding problem along the interface between prosthesis and host tissue. Authors conclude that the bone loss is dependent of Young's modulus of the material used to compose the femoral prosthesis.

Weinans et al. (1992) evaluated the material stiffness of the prosthesis for components with and without cement to promote the fixation around the host tissue. Authors use a two-dimensional model coupled with a bone-remodeling model that uses mass strain energy density as mechanical stimuli. The authors found that high level stiffness material causes more resorption than flexible material, which leads for resorption process along the interface bone-prosthesis or bone-cement-prosthesis. Other point evaluated is the strain energy density along the femur. There are high-levels in interface and proximal portion when a flexible material is used to compose the femoral prosthesis, what makes impossible the utilization of this kind of material for that application.

Herrera et al. (2008) evaluate titanium alloy for a three-dimensional cementless prosthesis model. Authors found that there are more changes in first year after prosthesis installation. In the end of the analysis, proximal region (for lateral and medial side) is the portion more affected by stress shielding problem.

Other authors that study bone remodeling around the cementless prosthesis are Scannel and Prendergast (2009). They applied a bone-remodeling model based on damage mechanics combined with strain caused by load application. They use a three-dimensional model and evaluate different materials (cobalt-chrome alloy, titanium alloy and an elastic material with low level of stiffness). The higher and lower stiffness materials cause no favorable conditions for bone remodeling around prosthesis. As well as Herrera et al. (2008), modifications in bone densities distribution happen until the end of first year and become practically constant.

Yan et al. (2011) use bone-remodeling model proposed by Huiskes et al. (1992). Authors evaluate porous and solid titanium and cobalt-chrome alloy. As well as Huiskes et al. (1992), the results show that the mainly aspect for bone-remodeling adaptation around a femoral component is the Young's modulus value. Best result are found when porous titanium is used while the stiffness of cobalt-chrome alloy causes high-level resorption in proximal region.

Kwon et al. (2013) present other study where big changes in density distribution happen until the end of first year. Authors evaluate their bone-remodeling model, which uses strain as mechanical stimuli. Just cobalt-chrome is used to evaluate the remodeling process.

As was posted, several authors evaluated the bone-remodeling process around a cementless component, applying different materials. This study aims the numerical evaluation of bone tissue behavior around a total hip prosthesis. For evaluate the adaptation process is used Stanford's isotropic bone-remodeling model (Jacobs, 1994). It is evaluated the effects of material stiffness of the cementless prosthesis used, which are the cobalt-chrome alloy, titanium alloy and a virtual material with Young's modulus similar to cortical bone. Other aspect verified is the stress distribution along the interface bone-prosthesis. For this, analysis run with the software Abaqus, using three-dimensional elements.

2 MATERIALS AND METHODS

This section presents bone-remodeling model, femur and prosthesis solid models used on this study, and finite element model with boundary conditions.

2.1 Bone remodeling process

We apply bone-remodeling process in two situations in this study. First situation is the phase before the THA, where the process is applied for an intact femur model. A heterogeneous densities field is obtained in the end of the first analysis. This field is “recovered” and used as initial conditions for second situation, which is the phase after THA. The complete process is presented in Fig. 1.

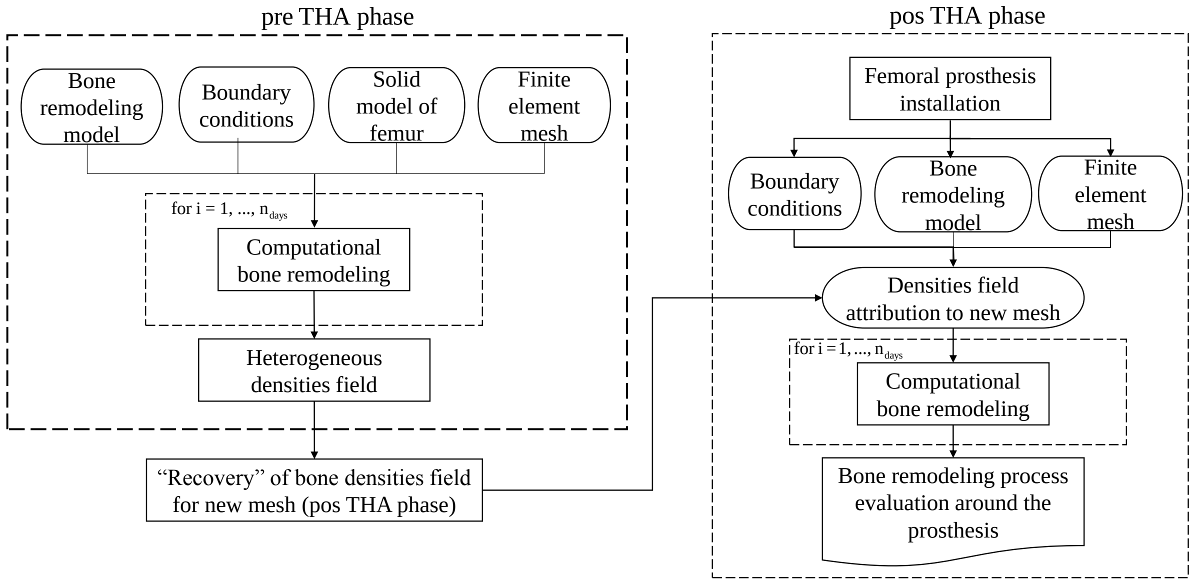

Figure 1. Flowchart of the bone-remodeling process studied

2.2 Stanford isotropic bone-remodeling model

Jacobs (1994) proposed an important bone-remodeling model. This model considers bone tissue as elastic, linear and isotropic behavior and its formulation is based on theory presented by Beaupré et al. (1990). Both studies use strain energy density as mechanical stimulus for modification of bone tissue properties. According to Beaupré et al. (1990), bone tissue is stimulated by a daily tissue level stress stimuli, ψ_t, where the rate of remodeling, $\dot{r}$, can be determined as

$$\dot{r} = \begin{cases} c\,[(\psi_t - (\psi_t^* - w))] & if\ \psi_t < (\psi_t^* - w) \\ 0 & if\ (\psi_t^* - w) \leq \psi_t \leq (\psi_t^* + w), \\ c\,[(\psi_t - (\psi_t^* + w))] & if\ \psi_t > (\psi_t^* + w) \end{cases} \tag{1}$$

on this case, ψ_t^* is the reference value for daily tissue stress stimuli and it is the central point in a region named dead zone (where there are not changes in bone tissue properties in this zone). Other variables are *c*, which is an empirical rate constant, *w* that is the half of dead zone interval

Proceedings of the XXXVIII Iberian Latin-American Congress on Computational Methods in Engineering
P.O. Faria, R.H. Lopez, L.F.F. Miguel, W.J.S. Gomes, M. Noronha (Editores), ABMEC, Florianópolis, SC, Brazil, November 5-8, 2017.

and finally, ψ_t is daily tissue stress stimuli and it is determined as (Beaupré et al., 1990; Jacobs et al., 1995)

$$\psi_t = \left(\sum_{days} n_i \overline{\sigma}_{t_i}^{m} \right)^{\frac{1}{m}}, \tag{2}$$

with n_i the load cycles number of load type *i*, $\overline{\sigma}_{t_i}$ is the bone tissue level effective stress value for that region associate with the load *i* and *m* is an empirical constant of the material.

With several experiments accomplished, Beaupré et al. (1990) concluded that material stress in a continuum level ($\overline{\sigma}$) can be associated with bone tissue level effective stress value ($\overline{\sigma}_{t_i}$), for a given apparent density (ρ) as

$$\overline{\sigma}(\rho) = \left(\frac{\rho}{\rho_c} \right)^2 \overline{\sigma}_{t_i}, \tag{3}$$

where ρ_c is the bone cortical density value. Thus, daily tissue level stress stimuli, ψ , associated with effective stress ($\overline{\sigma}$) can be written as (Jacobs et al., 1995)

$$\psi = \left(\sum_{days} n_i \overline{\sigma}_i^{m} \right)^{\frac{1}{m}}. \tag{4}$$

The material apparent stress in a continuum level is defined as

$$\overline{\sigma}_i = \sqrt{2EU_i}. \tag{5}$$

In this equation, U_i is the strain density energy value derivative of *i*-th load case and calculated by $U_i = \frac{1}{2}\varepsilon_i : C : \varepsilon_i$, with *C* the constitutive stiffness tensor of material and ε_i the strain tensor for *i*-th load case. In Eq. (5), *E* is the longitudinal Young's modulus associated to material density determined as

$$E(\rho) = b(\rho)\rho^{\beta(\rho)}. \tag{6}$$

For this study

$$E[MPa] = E(\rho) = b\rho^{(\beta)} = \begin{cases} 2014\,\rho^{2,5} & se\ \rho \le 1{,}2\ g/cm^3 \\ 1763\,\rho^{3,2} & se\ \rho > 1{,}2\ g/cm^3 \end{cases}, \tag{7}$$

with b and β functions of the Stanford model defined as a Young's modulus power law in terms of density. As well as Young's modulus, Poisson's ratio is defined according to density local value as

$$\nu = \begin{cases} 0{,}2 & se\ \rho \leq 1{,}2\ g/cm^3 \\ 0{,}32 & se\ \rho > 1{,}2\ g/cm^3 \end{cases}. \tag{8}$$

The density evolution rate ($\dot{\rho}$) is directly associated to specific surface area (S_v) for bone tissue apposition and resorption. Thus, it is very important to determine the available bone quantity for bone remodeling per unit of volume. Corso (2006) used data from a tomography to present a specific surface area approximation in terms of apparent density, ρ , as

$$S_v = -0{,}07 + 8{,}1\rho - 7{,}2\rho^2 + 5{,}1\rho^3 - 2{,}1\rho^4 + 0{,}23\rho^5 . \tag{9}$$

The density evolution rate is a function that depends of the rate of remodeling ($\dot{r}$) and specific surface area (S_v) and can be determine as

$$\dot{\rho} = k\, S_v \dot{r} \rho_c . \tag{10}$$

where k is the remodeling active surface (Jacobs, 1994; Doblaré and García, 2001). Thus the actualized density can de be obtained as

$$\rho^{n+1} = \rho^n + \dot{\rho}^n \Delta t . \tag{11}$$

In this equation, ρ^{n+1} is the actualized density value, ρ^n is the current value for densify for each integration point of finite element in mesh and Δt is the time interval referent to bone-remodeling process period for one load cycle.

After density update, a new load case starts and mechanical properties of femur are re-calculated. This characterizes the bone-remodeling incremental process. Table 1 presents necessary constants for Stanford isotropic bone-remodeling.

Table 1. Constants used in computational analyses of Stanford model (1994)

Parameters	Value	Unit
c	2.0×10^{-5}	(mm/day)/(MPa/day)
ψ_t^*	50.0	MPa
m	4.0	-
n_i	3000	Cycles/day
w	$0.125\times\psi_t^*$	MPa
ρ_c	2.0	g/cm³
Δt	7	Day
k	1.0	-

2.3 Finite element model

Before the THA, the analysis is made using three-dimensional solid model of a human femur (Grabcad, 2015) presented in Fig. 2a and the respective mesh (Fig. 2b).

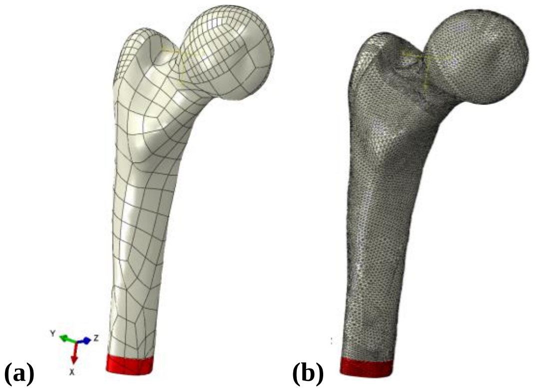

Figure 2: Solid (a) and FEM (b) models.

Finite element model is simulated in software Abaqus 6.12-1 (Abaqus, 2012) and is constituted by 490,570 linear tetrahedral elements (named C3D4) and 91,712 nodes. The load condition (Gubaua, 2016; Dicati, 2015) applied is presented in Fig. 3. This is developed using the load intensities presented by Beaupré et al. (1990), the areas of distributed load application on femoral head presented by Greenwald and Haynes (1972) and the directions and areas of load application on greater trochanter presented by Bagge (1999). Six loads compose the load condition, which characterizes a gait step and are derivative from two main sources. First, from the compression of femoral head due the contact with acetabulum. Second source is the muscle tractions forces that happen on greater trochanter. Table 2 presents the intensity and orientation of loads applied on femur model. Homogeneous boundary conditions of Dirichlet are applied in distal surface of the solid with elastic, isotropic and linear behavior united in medial portion of femoral diaphysis. This is made to avoid the stress concentration. Analysis starts with a homogeneous density value of the 1.0e-6 kg/mm³.

Table 2. Intensity and orientation of load applied on proximal human femur in 3D analysis.

Load	Intensity (N)	Orientation (grades)[1]
Compression – 1	1158	Pressure (normal to surface)
Compression – 2	2317	Pressure (normal to surface)
Compression – 3	1548	Pressure (normal to surface)
Traction – 1	351	27,53; 29,3; 59.65
Traction – 2	703	-5,933; 2,848; 39,29
Traction – 3	468	23,28; -27,93; 62,17

[1]Coordinate system is orientated with x-axis in lateral-medial direction, y-axis anterior-posterior direction and z-axis for lower-upper direction.

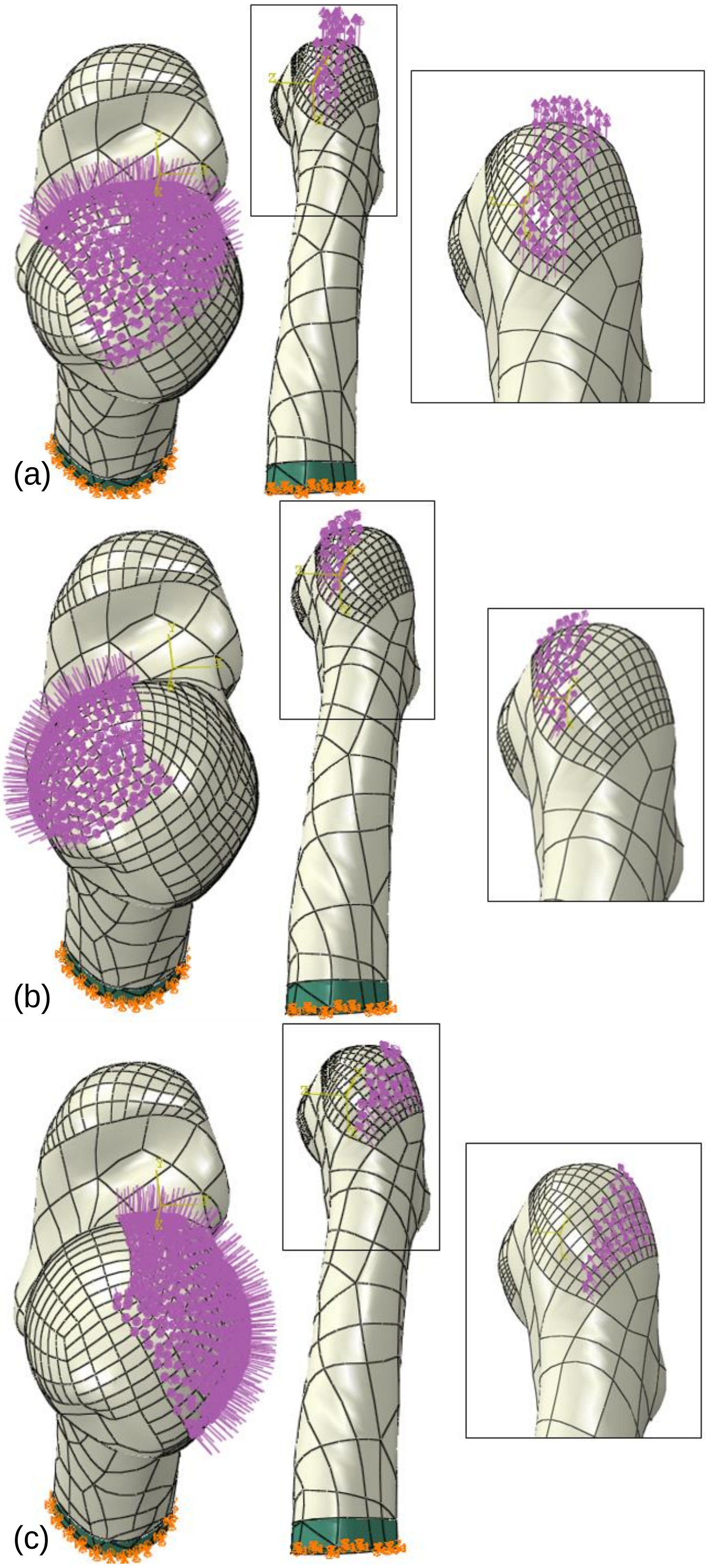

Figure 4: Load condition (Gubaua, 2016; Dicati, 2015) that simulates a gait composed by the initial moment of the gait (a) and abduction (b) and adduction (c) movements.

For analyses after THA, it is used the model presented in Fig. 4a. Prosthesis model (Grabcad, 2105) is presented in Fig. 4c. Three metallic materials are used and the properties are presented on the Table 3. First one is the cobalt-chrome alloy. Second material is titanium alloy and the last one is called virtual with similar properties to cortical bone. The yield strength of virtual material is defined using a map of mechanical properties of several materials, which relates Young's modulus and mechanical strength (Ashby, 2011). Bone/prosthesis interface is considered totally bonded.

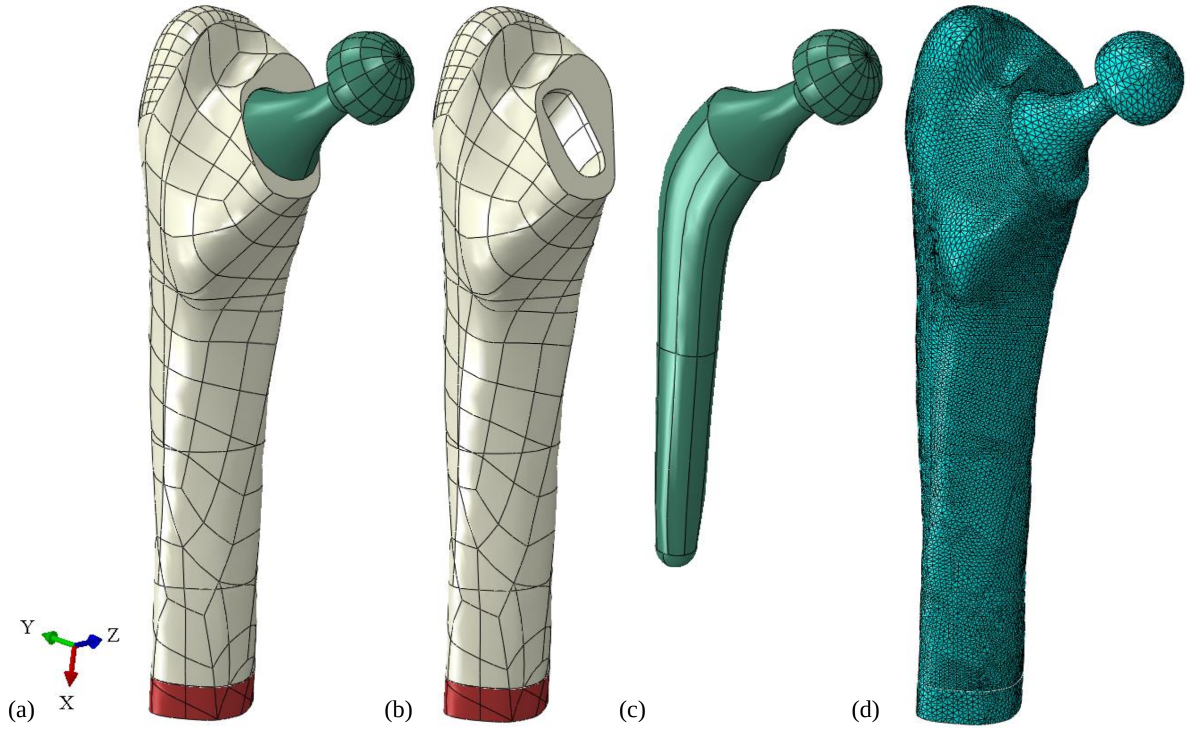

Figure 4: Model after THA (a), femoral cavity with solid united in diaphysis (b), prosthesis (c) and (d) discretized models.

Table 3. Metallic material used to simulate the prosthesis material.

Material	Yield strength (MPa)	Young's modulus (MPa)	Poisson's ratio
Cobalt-chrome	1606	210,000	0.3
Titanium	1034	120,000	0.3
Virtual	100	20,000	0.3

The same boundary conditions used to obtain the initial density distribution are applied after prosthesis installation, with the difference of the compression loads that are applied on prosthesis. 471,357 linear tetrahedral elements and 89,242 nodes compose finite element mesh (Fig. 4d). Initial density is "recovered" from equilibrium distribution before the THA. For this, it is developed a set of routines in software Matlab. "Recovery" process is done in two steps. First, a sphere with arbitrated radius is defined for each node in old mesh (femur model). Second, all coordinates of new mesh (femur with stem model) are evaluated in relation to coordinates of old mesh. This works like a patch, where the new nodal density value, for new mesh, is evaluate through a weighted average of the elementary densities inside this patch. After this, a simple nodal average is made to determine the elementary values.

Gruen et al. (1979) method is used to evaluate the bone mass variation (Fig. 5). This model divide the anteroposterior view in seven regions.

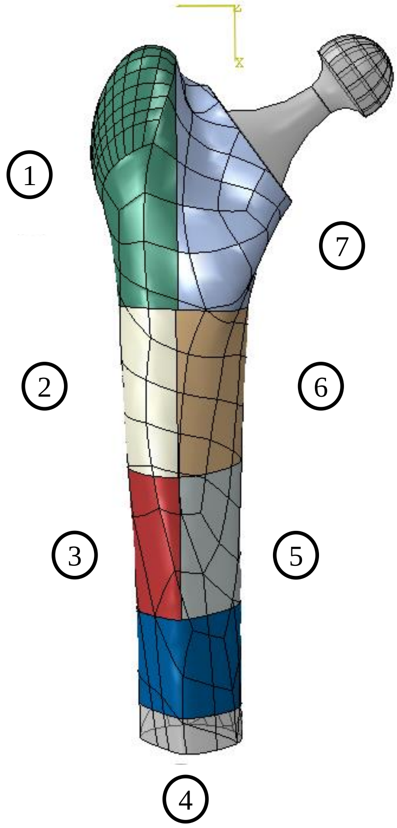

Figure 5: Gruen zones posted in femur with prosthesis model. Posteroanterior view.

2.4 Mechanical properties of bone tissue

Mechanical properties of bone tissue (trabecular and cortical) are presented on the Table 4.

Table 4. Mechanical properties of bone tissue.

Material	Properties	Value (MPa)	Reference
Cortical tissue	Maximum Traction	151	Doblaré and García (2003)
	Maximum Compression	-224	
Trabecular tissue	Maximum Compression	-80	Doblaré and García (2003)

3 RESULTS AND DISCUSSION

Figure 6a presents the final density distribution of Stanford's isotropic bone-remodeling model. This distribution characterizes the main morphological aspects of a real femoral density distribution like medial and lateral corticals, characteristic trabecular density along the greater trochanter and femoral head, Ward's triangle and medullary cavity. The distribution "recovered" and applied on mesh pos THA phase is presented in Figure 6b.

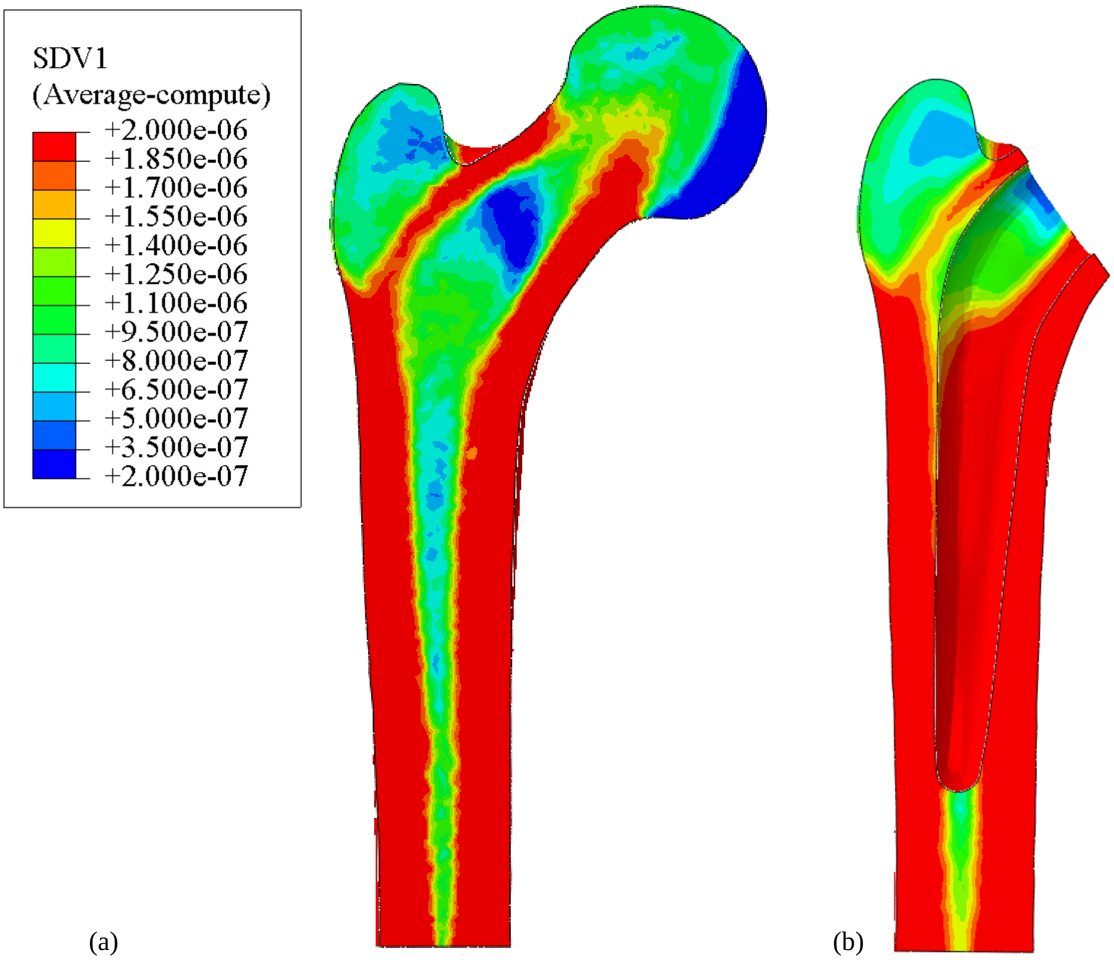

Figure 6: Density distribution (kg/mm³) before the THA (a) and recovered (b).

Figure 7 presents the results for 5 (five) years of analysis for bone-remodeling process around a component manufactured with cobalt-chrome alloy. Figure 7 (a) presents the bone mass variation (BMV) in percentage for each Gruen zone (GZ) as

$$BMV(\%) = \left(\frac{(ABM - IBM)}{IBM} \right) * 100, \tag{12}$$

with *ABM* the actual bone mass and *IBM* the initial bone mass for femur with prosthesis model. Fig. 7 (b) and 7 (c) are the initial and final bone density distributions (SDV1 in kg/mm³).

Final bone distribution (Fig. 7 (c)) shows the bone adaptation due to the stress shielding phenomenon. It is clear that the use of a prosthesis with a material stiffer than bone tissue will produce low-levels of load transmission in proximal portion of the model (GZ1 and GZ7), which causes the biggest level for bone resorption in adaptation process. Both lateral (GZ2 and GZ3) and medial (GZ5 and GZ6) corticals in femoral diaphysis have low variation when it is compared with initial distribution (up to 4%), but in a smaller level for medial cortical. Compression loads applied on the head of femoral prosthesis are dissipated directly on host tissue in distal portion of the component, which causes the bone pedestal formation (GZ4). This is a bone tendency to support the loads applied on the component beyond the bone resorption in proximal portion. The higher stiffness of the prosthesis material, the higher is the tendency of bone compaction in GZ4.

Bone mass variation (Fig. 7 (a)) is similar with results presented in literature, where there are more variation in first two years, becoming practically constant after that (Kwon et al., 2013; Scanell and Prendergast, 2009; Herrera et al., 2008; Jake and Scott, 1996). Although proximal portion (GZ1 and GZ7) has not found a stable distribution, the variation after two years is less than before, according to the references.

Figure 8 presents the results for bone adaptation around a prosthesis manufactured with titanium alloy. Figure 8 (a) presents the bone mass variation, while Fig 8 (b) and 8 (c) present the initial and final densities distribution (SDV1 in kg/mm^3). Stress shielding phenomenon has a similar behavior when it is compared with first material. A low-level of load transmission in proximal host tissue causes a bone resorption process in GZ1 and GZ7, nevertheless it is less aggressive when compared with cobalt-chrome component. Gruen zones that belong to diaphysis femoral do not have large variations (up to 2%) and bone pedestal can be visualized in GZ4 as a bone answer due the load application.

Likewise first material, bone tissue adaptation, leading by bone resorption, has the most part of variation in the end of the second year. However, there is an improvement in bone adaptation when a material more flexible is used.

Figure 9 presents the results for prosthesis composed with virtual material. Bone mass variation, initial and final densities distribution (SDV1 in kg/mm^3) are presented in Fig. 9 (a), 9 (b) and 9 (c) respectively. This material has a totally different behavior. There is more load transmission than others material analyzed, which helps bone maintenance in proximal region (mainly in GZ7). Furthermore, this material causes the lowest level of the bone adaptation along the host tissue. Large part of forces applied in femoral head of the prosthesis are transmitted in proximal portion. Lateral and medial corticals have a small variation (less than 2 %) and bone pedestal is visually imperceptible.

The less material stiffness, the less is the difference between materials in interface and thus the load transmission is favored, which would lead to the choice of virtual material to compose the prosthesis. However, there is at least one aspect very important to verify the materials before to indicate the best one for the application studied.

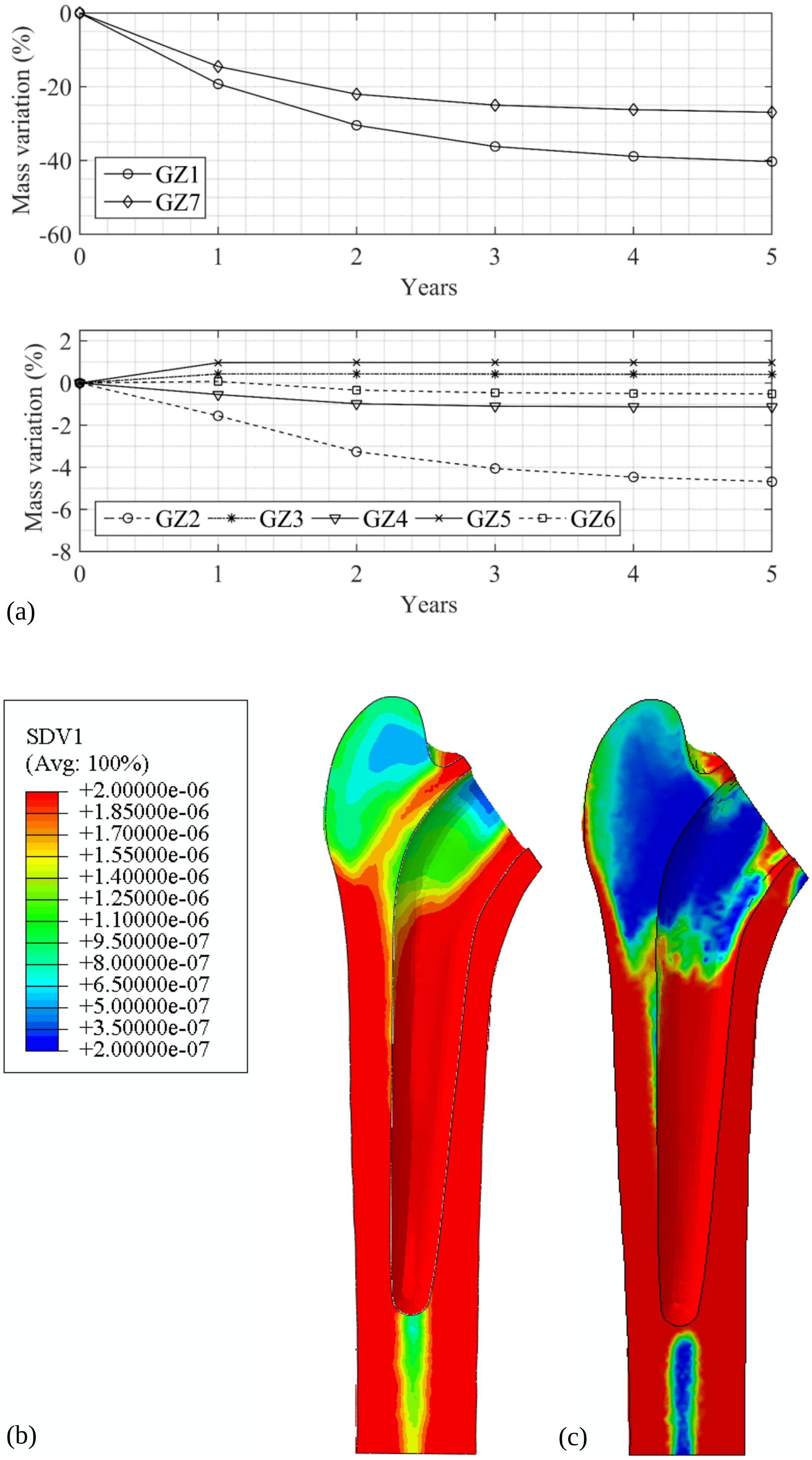

Figure 7: Results for one remodeling analysis around the prosthesis manufactured by cobalt-chrome alloy: (a) bone mass variation (%) and initial (b) and final (c) densities distribution (SDV1 in kg/mm³).

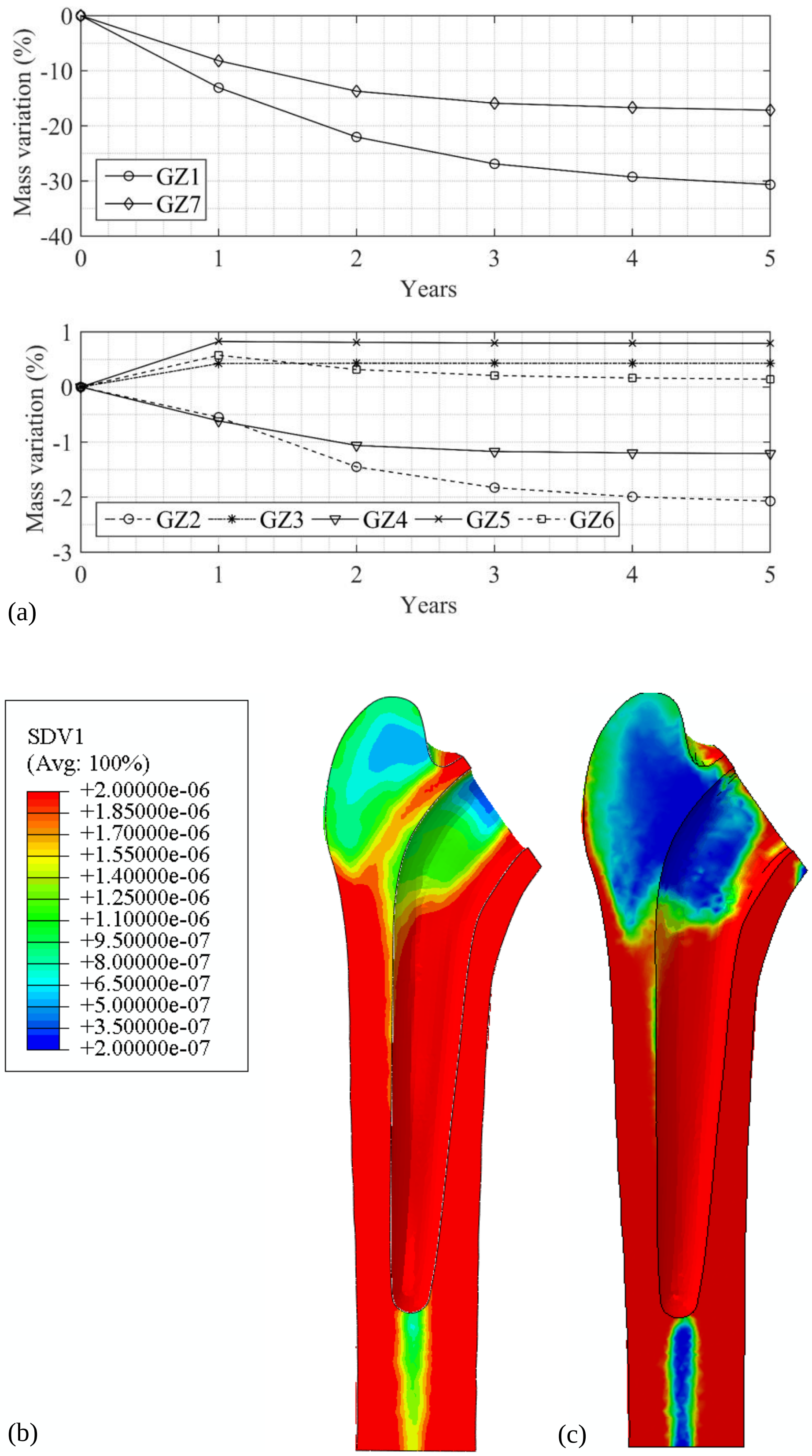

Figure 8: Results for one remodeling analysis around the prosthesis manufactured by titanium alloy: (a) bone mass variation (%) and initial (b) and final (c) densities distribution (SDV1 in kg/mm³).

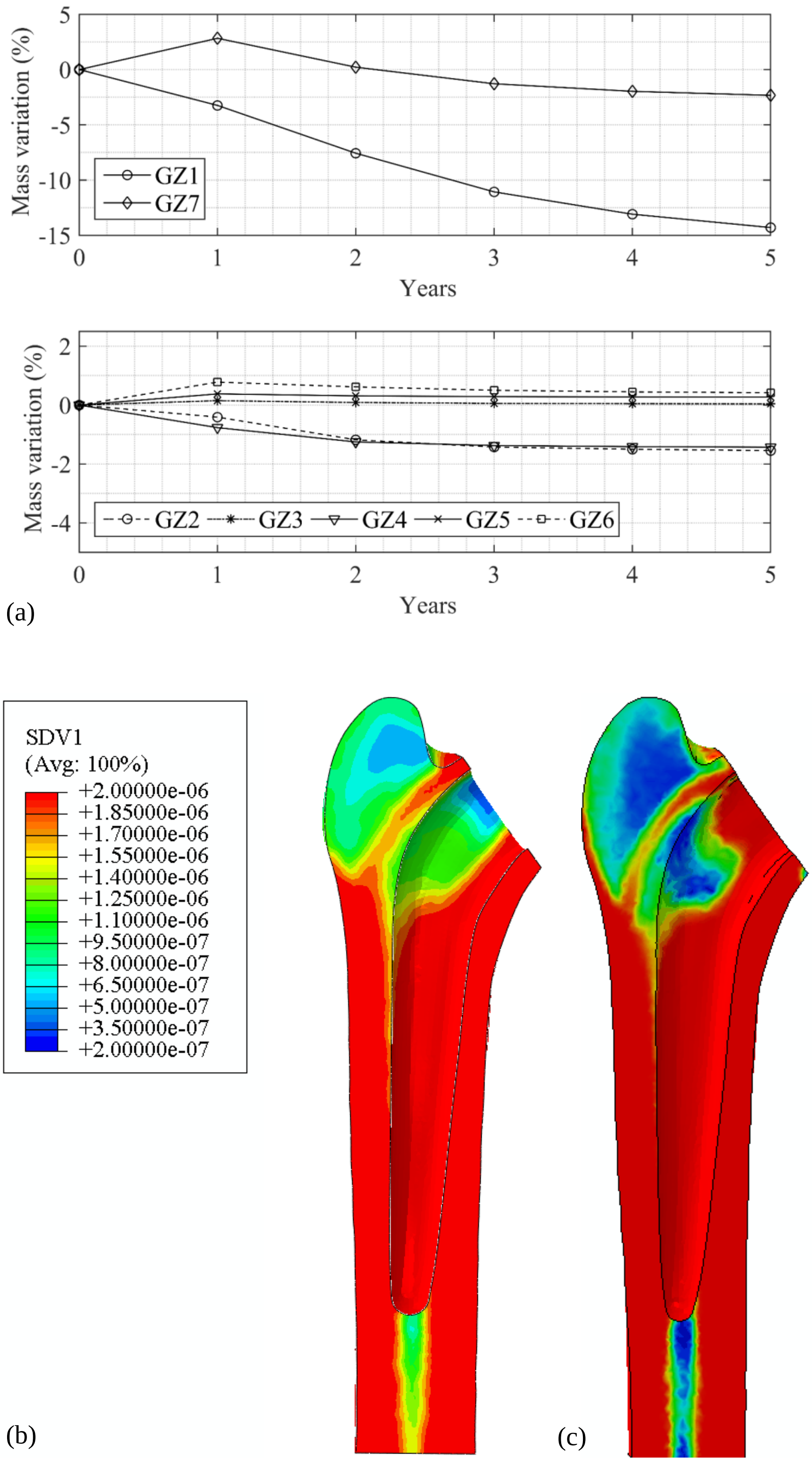

Figure 9: Results for one remodeling analysis around the prosthesis manufactured with virtual material: (a) bone mass variation (%) and initial (b) and final (c) densities distribution (SDV1 in kg/mm³).

Second aspect evaluated here is the stress field that occurs in interface and along the prosthesis. Likewise the stress shielding, stress field can compromise the success of the process. Those values can lead to the failure or even the fracture for both bone tissue and prosthesis material. The maximum and minimum principal stress values are verified to bone tissue due to the brittle behavior. Von Mises yield criterion is verified for stress distribution along the prosthesis. Table 5 presents the stress values that occur in the host bone in interface and Fig. 1 presents the stress field distribution along the prosthesis.

Table 5. Stress values that occur in bone interface.

Material		Stress (MPa) in interface	
		Initial	Final
Cobalt-chrome alloy	Max. principal	40.23$^{\infty}$	40.57$^{\infty}$
	Min. principal	-32.07$^{\infty}$	-31.86$^{\infty}$
Titanium alloy	Max. principal	35.86$^{\infty}$	36.57$^{\infty}$
	Min. principal	-37.59*	-38.24*
Virtual material	Max. principal	59.19*	55.05*
	Min. principal	-68.45*	-65.13*

$^{\infty}$ Stress occurs in distal portion of the interface; *Stress occurs in proximal portion of the interface.

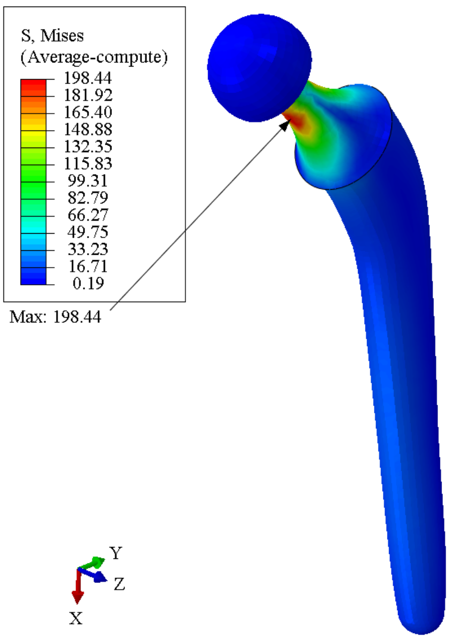

Figure 11: von Mises stress (MPa) distribution along the prosthesis.

None material used in prosthesis causes the bone tissue failure in interface. Flexible materials produce stress in proximal portion of the interface, what increase the load transmission and decrease the intensity of stress shielding phenomenon. Rigid materials produces stress in distal portion of the interface, what decreases the load transmission and increases the stress shielding. For material prosthesis, virtual material causes prosthesis failure in first step of the analysis (Table 4), what makes it impossible for this application.

4 CONCLUSIONS

Bone-remodeling adaptation around a femoral prosthesis is evaluated for different metallic materials. A main phenomenon that happens in this situation is called stress shielding, which is improved according to the material stiffness of the prosthesis. Bone adaptation is more aggressive for prosthesis manufactured with cobalt-chrome alloy, because the big difference between prosthesis stiffness and bone tissue stiffness. This causes a poor load transmission in proximal portion of the interface, which leads for the biggest bone resorption between materials evaluated. Flexible materials improve the load transmission, but the stress field caused along the prosthesis can cause the materials failure as visualized for virtual material. For the application evaluated in this study, the best choice is the titanium alloy. This material causes a less stress shielding in proximal region when compared with cobalt-chrome alloy, and supports the stress caused due the load condition in artificial hip joint.

Stanford bone-remodeling model produces effects that observed in clinical results. However, this model is the main answer to understand the changes in bone densities distribution after two years and does not meet a stable configuration in proximal portion. Distributions are presented with post-processing tool available in Abaqus software, improving the quality of results. Original approach, that is, formulation presented by Jacobs (1994), leads for a non-continuum distribution, which is characterized for a pattern similar to a chessboard, named checkerboard. This leads to a non-stable configuration. When a method to control is applied, as stress field smoothing method, this model leads to a stable configuration (Silva et al., 2015). Although the model presents this problem, results obtained in this study can be qualitatively compared with clinical ones.

The load conditions here presented is a simplification of the load condition that happens in a real situation. Just the gluteus muscles are assumed as muscle reaction and even so produces qualitatively results. Muscles as psoas major and illiacus, which are inserted in lesser trochanter, can be improve the results.

Therefore, even with the simplifications presented, FEM is a powerful tool to understand and evaluate biological processes, as bone remodeling, and to the development of components that can help people to have better quality of life again.

REFERENCES

Abaqus, v. 6.12-1. Dassault Systèmes, 2012.

Ashby, F. M., 2011. *Materials Selection in Mechanical Design*. Elsevier.

Bagge, M., 1999. *Remodeling of bone structures.* PhD Thesis, Technical University of Denmark.

Beaupré, G.S., Orr, T., Carter, D. R., 1990. An approach for time-dependent bone modeling and remodeling – Theoretical development. *Journal of Orthopaedic Research*, vol. 8. Pp. 651-661.

Corso, L. L., 2006.*Aplicação de procedimentos de otimização e remodelamento ósseo na simulação e análise de problemas de biomecânica*. Master Thesis, Federal University of Rio Grande do Sul.

Dicati, G. W. O., 2015. *Análise comparativa entre os modelos de Stanford isotrópico e anisotrópico para remodelação óssea utilizando o método dos elementos finitos 2d e 3d.* Master Thesis, Federal University of Paraná.

Doblaré, M., García, J. M., 2001. Application of an anisotropic bone-remodelling model based on a damage-repair theory to the analysis of the proximal femur before and after total hip replacement. *Journal of Biomechanics,* vol. 34, pp. 1157-1170.

Doblaré, M., García, J. M., 2003. On the modeling bone tissue fracture and healing of the bone tissue. *Acta Cientifica Venezolana,* vol. 54, pp. 58-75.

Gubaua, J. E., 2016. *Análise numérica da influência da rigidez de próteses femorais no processo de remodelação óssea associado à técnica cirúrgica de Artroplastia total de quadril.* Master Thesis, Federal University of Paraná.

Grabcad. Avaliable in: www.grabcad.com. Access in: 25/11/2014 and 10/03/2015.

Greenwald, A.S., Haynes, D.W., 1972. Weight-bearing areas in the human hip joint. *The Journal of Bone and Joint Surgery*, vol. 54, pp. 157-163.

Gruen, T. A., McNeide G. M., Amstutz H. C., 1979. "Modes of failure" of cemented stem-type femoral components: a radiographic analysis of loosening. *Clinical Orthopaedics and Related Research*, vol. 141, pp. 17-27.

Herrera, A., Panisello, J. J., Ibarz, E., Cegoñino, J. A., Gracia, L., 2008. Densitometric and finite-element analysis of bone remodeling further to implantation of na uncemented anatomical femoral stem. *Revista de Cirurgía Ortopédica y Traumatológica*, vol. 52, pp. 269-282.

Huiskes, R., Weinans, H., Dalstra, M., 1989. Adaptative bone remodeling and biomechanical design considerations for noncemented total hip arthroplasty. *Orthopedics*, vol. 12, pp. 1255-1267.

Huiskes R., Weinans, H., Rietbergen, B., 1992. The relationship between stress shielding and bone resorption around total hip stems and the effects of flexible materials. *Clinical Orthopaedics and Related Research*, pp. 124-134.

Jacobs, C. R**.**, 1994. *Numerical Simulation of Bone Adaptation to Mechanical Loading*. PhD Thesis, Stanford University.

Jacobs, C. R., Levenston, M. E., Beaupré, G. S., Simo, J. C., Carter, D. R., 1995. Numerical instabilities in bone remodeling simulations: the advantages of a node-based finite element approach. *Journal of Biomechanics*, vol. 28, pp. 449-459.

Jake, W. L., Scott, D.F., 1996. Current concepts and review. Total hip arthroplasty with hydroxyapatite-coated prostheses. *The Journal of Bone and Joint Surgery*, vol. 78, pp. 1918-1934.

Kwon, J. Y., Naito, H., Matsumoto, T., Tanaka, M., 2013. Estimation of change of bone structures after total hip replacement using bone remodeling simulation. *Clinical Biomechanics*, vol. 28, pp. 514-518.

Ministério da Saúde (2014). *Into promove mutirão de cirurgias de quadril***.** Avaliable in: http://portalsaude.saude.gov.br/index.php/cidadao/principal/agencia-saude/14912-into-promove-mutirao-de-cirurgias-de-quadril. Access in 14/10/2015.

Scanell, P. T., Prendergast, P. J., 2009. Cortical and interfacial bone changes around a non-cemented hip implant: Simulations using a combined strain/damaged remodeling algorithm. *Medical Engineering & Physics*, vol. 31, pp. 477-488.

Silva, J., Gubaua, J. E., Dicati, G. W. O., Pereira, J. P., 2015. Análise de diferentes metodologias para evitar a formação do padrão similar de checkerboard em uma análise de remodelação óssea bidimensional. In. *XXXVI Iberian Latin-American Congress on Computational Methods in Engineering (CILANCE 2015).*

Weinans, H., Huiskes, R., Grootenboer, H. J., 1992. Effects of material properties of femoral hip components on bone remodeling. *Journal of Orthopaedic Research*, vol. 10, pp. 845-853.

Yan, W., Berthe, J., Wen, C., 2010. Numerical investigation of the effect of porous titanium femoral prosthesis on bone remodeling. *Materials and Design*, vol. 32, pp. 1776-1782.